

## FUNNELING EXPERIENCE AT LOS ALAMOS: EXPERIMENTS AND DESIGNS\*

Andrew J. Jason, Ken F. Johnson, and Subrata Nath  
Los Alamos National Laboratory, Los Alamos, NM 87545

### I. INTRODUCTION

Modern linacs are capable of accelerating high-current low-emittance beams input above a minimum energy. However, the ability of ion sources to produce such beams and the ability of low energy structures to accelerate high currents to this minimum energy is lacking. Funneling is a method of combining two or more beams to overcome this limitation. The process is simply illustrated in the sketch of Figure 1. It is very important to

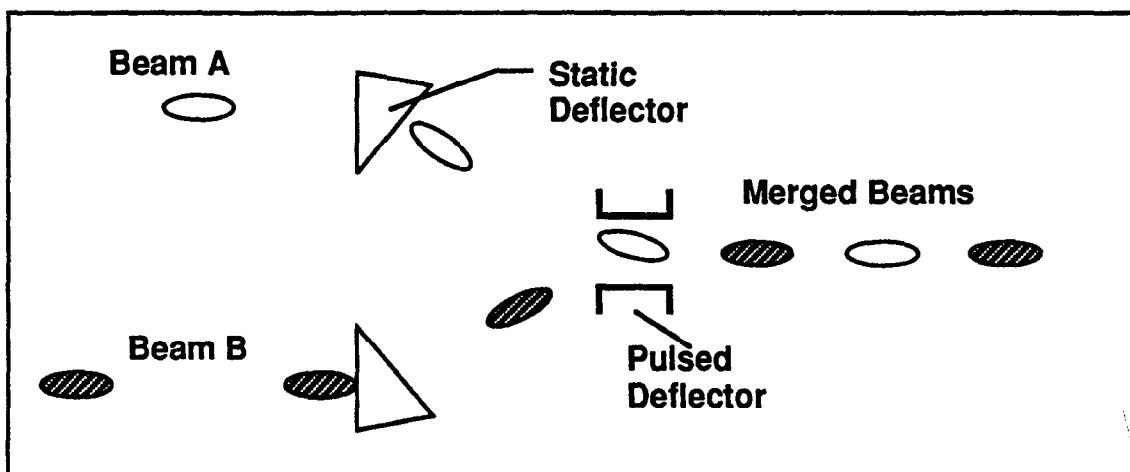


Figure 1. Schematic of basic funneling concept. Two separate beams, A and B, are merged by interleaving beam pulses to produce a beam of doubled frequency. The element labeled "pulsed deflector" must deflect alternate beam pulses in opposite directions.

note that the phase space of the two beams to be combined is not merged, in violation of Liouville's theorem. Instead beam micropulses from two sources are interleaved in time. It is also important to note that the micropulse frequency has doubled over that of the separate sources and must be accommodated by the linac following the funnel. Thus if the two funneled beams were accelerated by 400 MHz linacs, further acceleration must be done by an 800 MHz (or higher) linac. Other concepts are possible, but we concentrate on the one presented as the most feasible. The inclusion of further elements than shown in Figure 1 is needed for a practical device. In particular, the presence of both longitudinal and transverse focusing elements are crucial to device performance as are adequate diagnostic elements.

To attain the high peak currents needed for Los Alamos projects, such as the Ground Test Accelerator (GTA) [1], Accelerator Production of Tritium (APT) [2], Accelerator Transmutation of Waste (ATW) [3], or the 5 MW upgrade to the National Center for Neutron Research (NCNR) [4], a funneling scheme is needed. In these projects we consider funneling of two beams with peak currents of up to 100 mA and transverse emittances of the order of  $0.02\pi$  cm mrad, rms normalized.

In this article we will discuss a funneling experiment done at Los Alamos and briefly mention a program at another institution that has demonstrated the concept. We will also discuss the funnel design for APT, now undergoing conceptual design.

---

\*Work Supported by the US Department of Energy, Office of Defense Programs.

## II. THE ATS FUNNEL EXPERIMENT

To demonstrate the funneling concept, a team at Los Alamos constructed a prototype device that explored the main issues inherent in the concept. Although we were certain of the *in principle* feasibility of funneling, it remained to be shown that, in practice, we could maintain emittance and steering control. Additionally, it was important to demonstrate the implementation of a pulsed deflector, which in this case took the form of a specialized rf cavity constructed to provide a deflecting mode by an rf field. We were also able to test the performance of several diagnostic systems that had recently been developed.

We had available a device called the Accelerator Test Stand (ATS) that could produce over 40 mA  $H^-$  peak current with an rms normalized emittance near  $0.02\pi$  cm mrad at an energy of 5 MeV. The ATS consisted of a source, a radio-frequency quadrupole accelerator, and a drift tube linac (DTL). The funnel experiment was placed immediately downstream of the DTL.

### A. Beam Characterization

Before going into detail about the equipment, we briefly discuss the diagnostics used to characterize the output beam during the various stages of the experiment. This is in contrast to the funnel permanent diagnostics that can measure only profile, position, and current. The diagnostics unit, known as the D-plate [5] is shown in Figure 2. At the

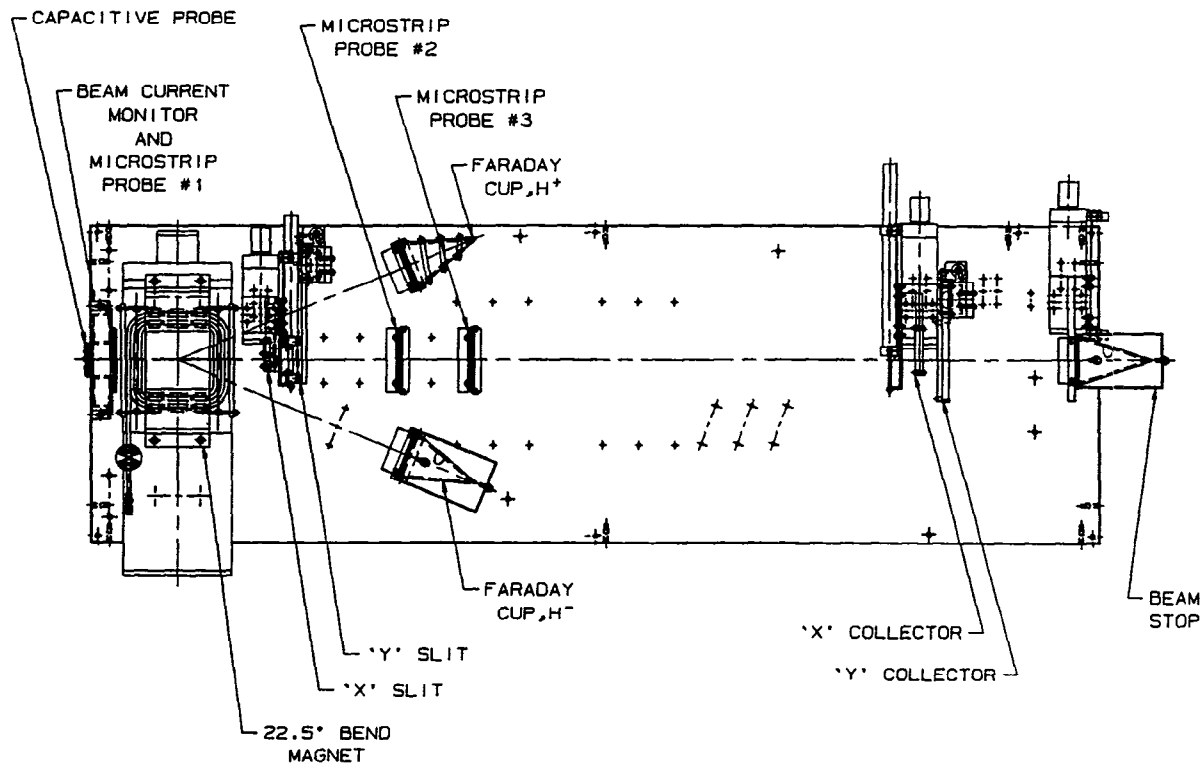


Figure 2. The GTA diagnostics plate. The length of the plate is 1.4 meters and beam direction is from left to right.

upstream end of the D plate an additional assembly is mounted that defines the intersection of the Laser Induced Neutral Diagnostic Approach (LINDA) [6]. LINDA uses very fast 532-nm laser pulses to neutralize a longitudinal segment of a beam pulse. By timing across the length of the D plate, the energy and phase of the segment can be determined. Hence, the projection of the beam distribution onto longitudinal phase space can be fully determined. In a second mode, measurement of the transverse phase space is accomplished. Here, the intensity of a beam micropulse is reduced by a long partially-neutralizing laser pulse so that measurement diagnostics are not damaged and so that space charge forces do not affect the beam distribution during flight across the D plate. The transverse measurement is done by scanning a pair of slits (labeled x slit and y slit in Figure 2) across the beam to define position and a pair of segmented collector electrodes downstream to define angle. Thus the entire four-dimensional transverse phase space can be explored with a resolution of 0.1 mm by 800  $\mu$ rad. The microstrip probes are short four-lobe directional-coupler pickups that determine beam position and are also used for timing. In both LINDA modes, unstripped beam is removed by a sweeping magnet shown in Figure 2.

As part of the diagnostics development program, sophisticated electronics modules were implemented and software developed for analysis of data. In particular a set of algorithms was established known as phase scans [7] to tune the linac and rf cavities. The resultant capabilities allowed complete characterization of beam from the linac and funnel.

- Distribution in longitudinal phase space - LINDA selects a narrow band of phase. Energy and phase values determined by timing signals from the microstrip probes. Signal is measured on a Faraday-cage beam stop.
- Distribution in transverse phase space - Slit and collector method defines angle and position of phase-space element. Collector signal measures relative intensity.
- Beam position - Difference measurements on the microstrip-probe lobes provides fast position information. The slit and collector measurements also gives centroid results on a slower time scale.
- Central energy and phase- Provided by microstrip-probe timing measurements.
- Beam current - Measured by a tape-wound-core toroid current monitor.

## B. Funnel Beamline

The funnel beamline is shown in Figure 3. The transverse focusing elements, labeled Q1 through Q15 were samarium-cobalt permanent-magnet quadrupole lenses with a nominal 1 cm bore. They maintained a periodic focusing structure similar to that of the linac to prevent emittance growth by space-charge effects. Four of the quads were mounted on remotely moveable stages and hence could be used to steer the beam. Four permanent-magnet dipoles provided the (distributed) function of the static deflector shown in Figure 1. Additionally, Q13 and Q14 provided deflection since the beam passed through them off center. The first two bunchers R1 and R2 were resonant at 425 MHz while R3 and R4 were 850 MHz cavities. These cavities provided the necessary longitudinal focusing at the initial and final beam frequencies. The pulsed-deflector function was provided by R5, a 425 MHz resonant cavity with parallel plate geometry. Cavity deflection was approximately 36 mrad at a peak input power of 90 kW. The beamline configuration was determined by beam-dynamic considerations to minimize emittance growth and to optimize steering control. The beam line was mounted on four separate plates for staged commissioning and the entire assembly was placed in a cylindrical vacuum vessel.

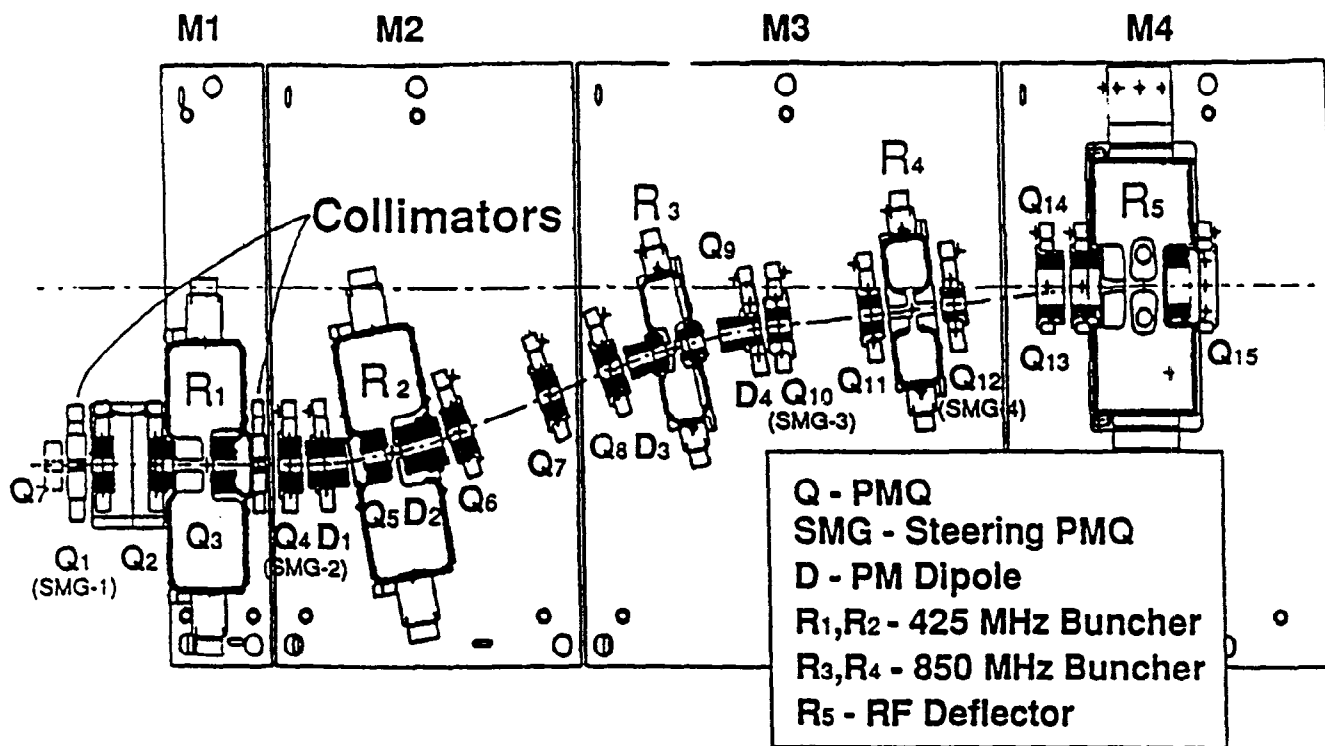


Figure 3. ATS funnel beamline schematic.

Several further permanent diagnostics, were incorporated into the funnel beamline. These consisted of eight microstrip probes to monitor position at critical points, approximately 90° in phase advance from the steering quads. Wire scanners at critical points in the beamline were used to measure the horizontal beam profile. A pair of toroid current monitors near the beamline extremes measured the transmission.

### C. Experimental Results.

The experiment was staged in four parts. First the linac was tuned using the phase-scan technique and emittances were measured. Because the ATS transverse emittances had increased by a factor of two, collimators at the start of the M1 segment were used to define the transverse emittances to 0.021 cm mrad rms normalized. The beam from the M1 plate was then characterized to set the R1 cavity value and check the collimated emittances. Next M2 and M3 were installed with similar tests including the full repertoire of the D plate. The remaining three buncher cavities were set using LINDA and beam loading measurements. Emittances and deflections remained good. Finally, M4 was installed and the entire beamline tested at peak currents of from 25 to 40 mA.

All experimental goals were achieved. Dynamics calculations had shown negligible emittance growth and this was verified by the experiment to within the experimental error (about 7%). Transmission through the funnel was 100% and steering control was achieved. The rf deflection technique functioned as expected.

Some of the major experimental results [8] are shown in Figures 4 and 5. Figure 4 shows that the optimum value of cavity phase relative to the beam is  $60^\circ$ . In other parameterizations, longitudinal and transverse emittances varied weakly with cavity power. The emittances varied with rf phase but were minimized at the  $60^\circ$  phase setting. In Figure 5, the result of allowing the beam to drift without emittance control is shown. Substantial emittance growth is seen due to space-charge forces; with the control of the funnel beamline, little emittance growth is seen.

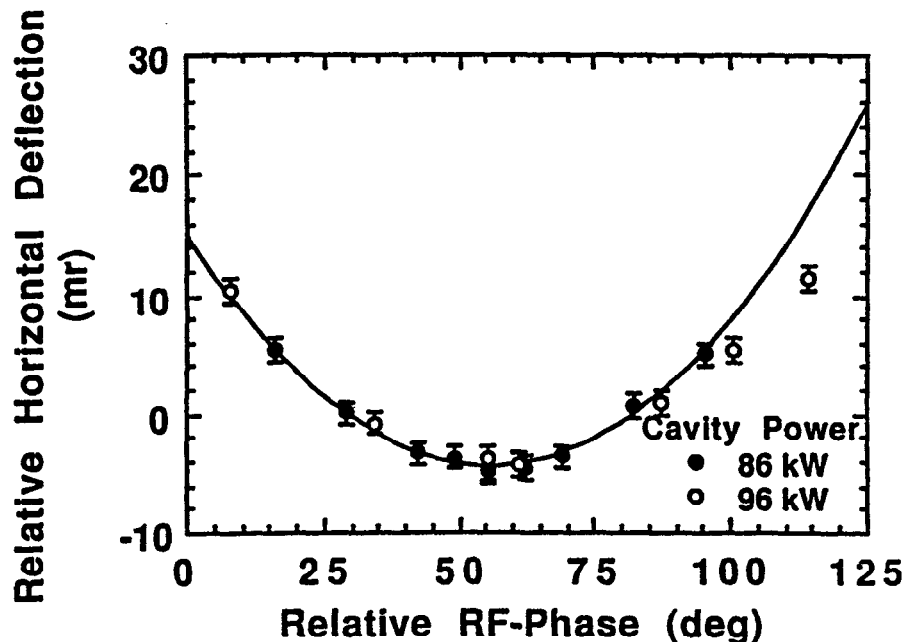


Fig 4. Horizontal deflection versus deflector cavity phase for two cavity powers. The optimum phase value was  $60^\circ$ . The deflection varied linearly with cavity power near the optimum values of phase and power.

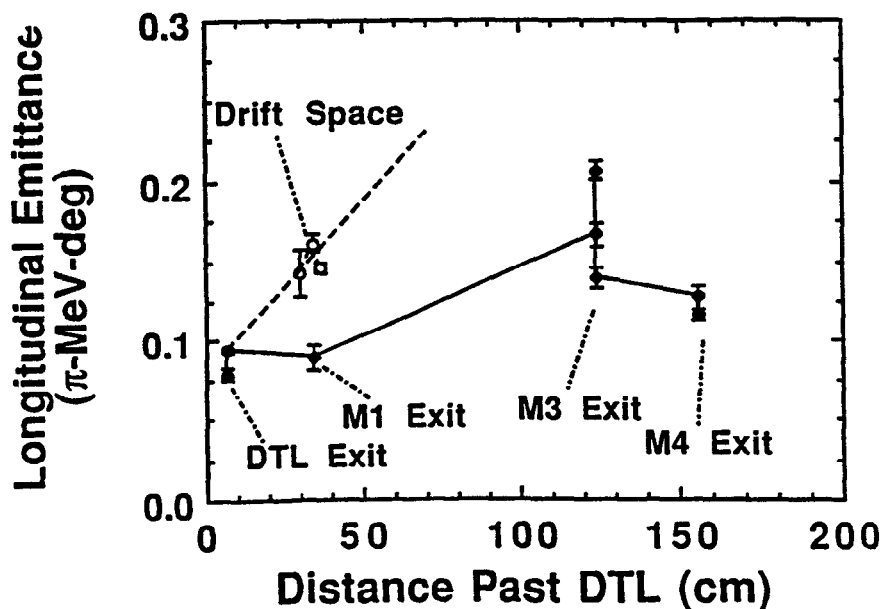


Fig 5. Longitudinal emittance versus distance from the DTL.

### III. THE MCDONNELL DOUGLAS FUNNEL EXPERIMENT

The ATS funnel experiment was a good demonstration of beam control. However, to convince the many skeptics of the viability of funneling a two-beam experiment would be important. Such an experiment was done by the McDonnell Douglas Missile Systems Company. Though we have as of yet little details of their results, the experiment showed that two beam funneling at 2 MeV resulted in little emittance growth. The funnel design used is shown in Figure 6.

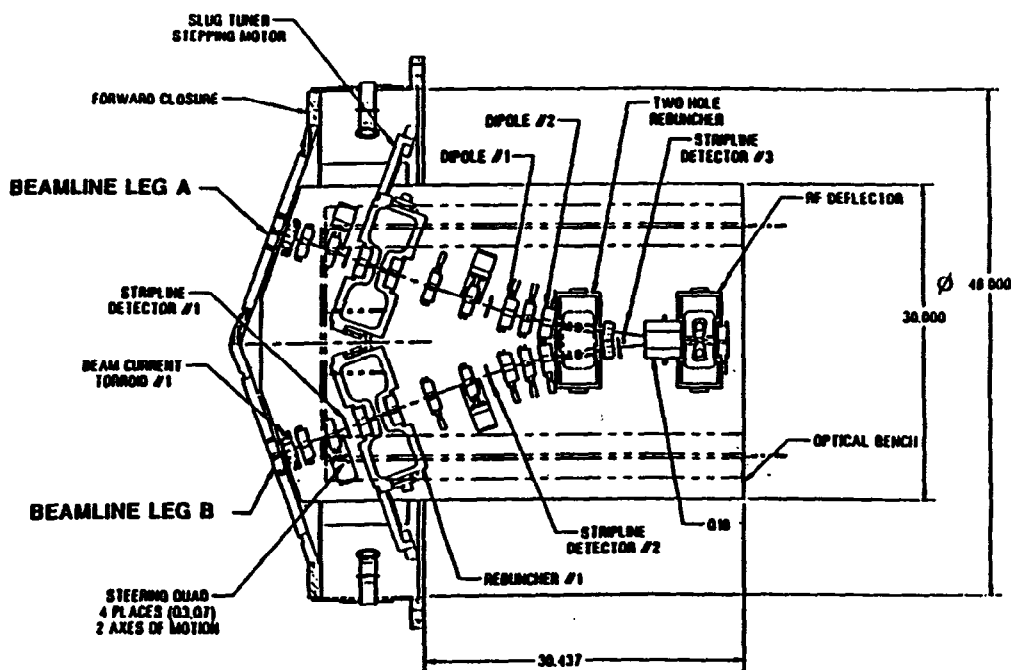


Figure 6. The McDonnell Douglas two-beam funnel beamline configuration.

One novel element in the design was the incorporation of a two-hole rebuncher. Note that in Figure 3, inclusion of a second leg would have resulted in an interference with buncher R4. The McDonnell Douglas experiment has resolved this and other engineering issues inherent in a two-beam funnel.

### IV. APT FUNNEL DESIGN

Based on the results of these experiments, a conceptual design of a funnel for the APT project has been proposed and is highly applicable to the NCNR project. Here the funneling energy is 20 MeV with a current in each leg of 100 mA. The resultant 200 mA beam will be matched to a 700 MHz bridge-coupled drift tube linac (BCDTL). The linacs will run at 100% duty factor. The input beam has transverse and longitudinal rms normalized emittances of  $0.023\pi$  cm mrad and  $0.22\pi$  deg MeV respectively. The rms bunch length on entrance to the funnel is  $5.5^\circ$  of 350 MHz rf phase, to be reduced to  $3.3^\circ$  at the output for matching into the 700 MHz BCDTL. The proposed beamline is shown in Figure 7.

The concept is similar to the other designs discussed. The bends are distributed among focusing elements to avoid substantial dispersion effects. Novel buncher cavities and a high-field deflector cavity are being designed. Note that an angle between the entrance and exit beam is required to provide clearance between the low-energy linacs.

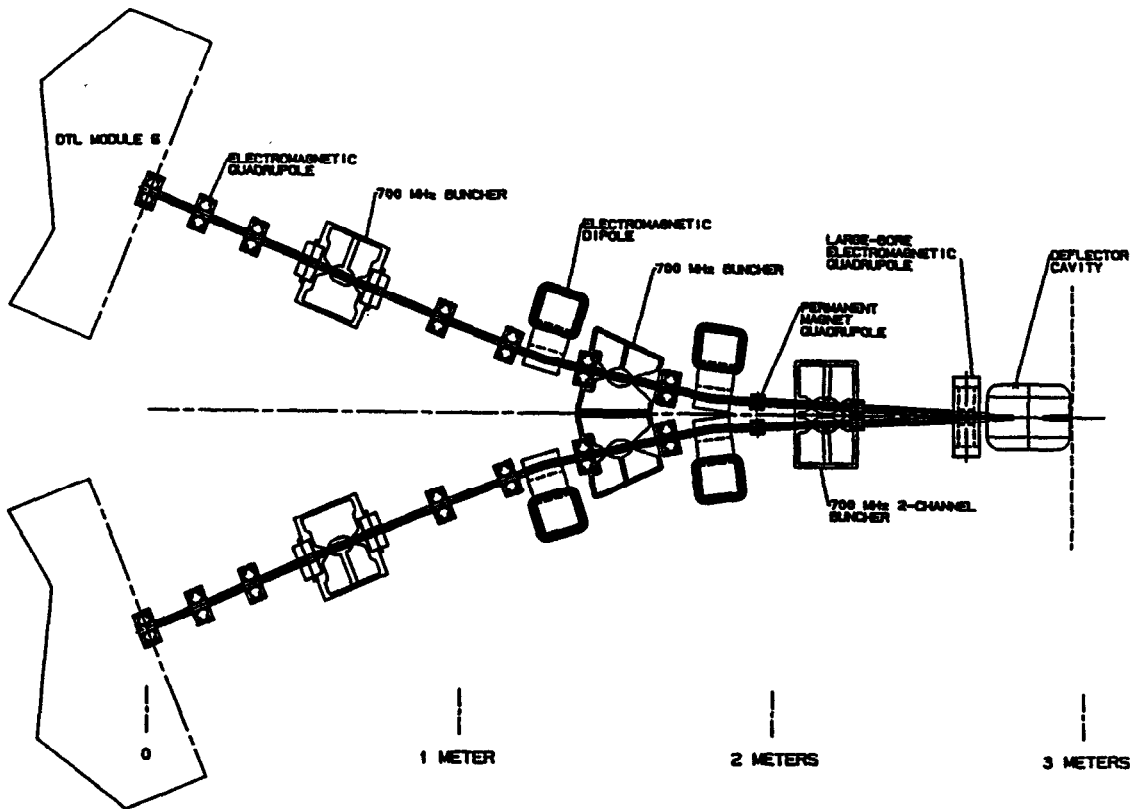


Figure 7. Layout of APT funnel conceptual design

A conceptual design for the deflector cavity has been proposed and the field distribution is shown in Figure 8. The deflecting voltage across the gap is 0.290 MV with a peak surface field of 1.3 Kilpatrick. The peak surface power density is some 60 W/cm<sup>2</sup>, representing a challenge in thermal transfer. The two hole buncher cavity has undergone preliminary design using the axially symmetric code SUPERFISH and needs further work with a three-dimensional code. Similarly to the McDonnell Douglas experiment, it is a two-gap device. The peak surface power density is about 40 W/cm<sup>2</sup> and the peak electric field is 1.4 Kilpatrick.

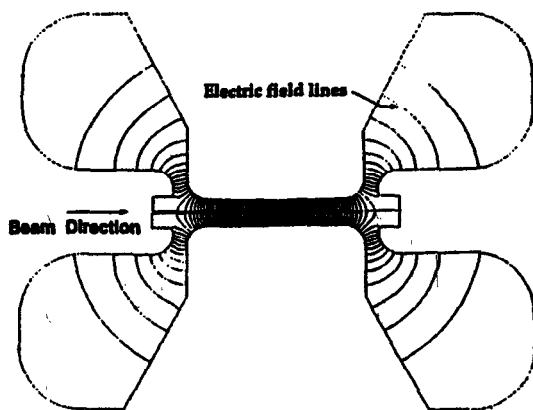


Figure 8. Sectional view of APT deflector cavity in the median deflecting plane. Electric field lines are shown. Each deflecting electrode is a rectangular prism wider in the diagram plane than in depth out of the plane. Otherwise, the diagram has azimuthal symmetry about a line perpendicular to the beam axis and in the plane of the diagram.

## V. SUMMARY

It seems evident that the major physics issues in funneling have been experimentally resolved. It is necessary to match and confine the beam well both longitudinally and transversely in order to prevent emittance growth. This is a lesson learned from general studies in beam dynamics that tell us that emittance is conserved when matching is good and the beam is either entirely dominated by focusing forces (as in these designs) or dominated by space charge forces, as would happen for a large weakly focused beam. This is seen clearly in Figure 5 where a beam that has been freely allowed to expand experiences severe emittance growth. It still remains, however, to demonstrate further acceleration to the final higher energy. This would demonstrate that the funneling process has not coupled phase planes, e.g., through chromatic terms, so that beam emittances grow upon further transport.

Further challenges involve rf cavity design and resolution of other engineering aspects of funnels for efficient operation.. In particular, heat transfer from the cavities for CW operation is critical. Superconducting devices may be appropriate in this regard. Additionally, diagnostic devices and rf control are issues with respect to minimizing beam losses.

## VII. REFERENCES

- [1] O. R. Sander, *et al.*, "Commissioning the GTA," *Proc. 1992 Linear Accelerator Conference*, Ottawa, August, 1992, p. 535.
- [2] "Accelerator and Beam Transport Design Information," APT Design Review, March 1993, Los Alamos Report LA-UR-93-980.
- [3] G.P. Lawrence, "High-Power Proton Linac for Transmuting the Long-Lived Fission Products in Nuclear Waste," *Nucl. Instr. and Meth.*, **B56/57** (1991) p. 1000.
- [4] A. J. Jason, "Overview of the NCNR Accelerator Studies," these proceedings.
- [5] J. D. Gilpatrick, *et al.*, "GTA Beam Diagnostics for Experiments 1B through 2D," Los Alamos National Laboratory report LA-UR-91-341 (April 1991).
- [6] W. V. Yuan, *et al.*, "Measurement of Longitudinal Phase Space in an Accelerated H<sup>-</sup> Beam Using a Laser-Induced Neutralization Method," *Nucl. Instr. and Meth.*, **A239** (1993) p. 381.
- [7] J. D. Gilpatrick, *et al.* "Synchronous Phase and Energy Measurement System for a 6.7 MeV H<sup>-</sup> Beam," *Proc. 1988 Linear Accelerator Conference*, Newport News, October, 1988, p. 134.
- [8] K. F. Johnson, *et al.*, "A Beam Funneling Demonstration: Experiment and Simulation," *Particle Accelerators*, 1992, **37-38**, p. 261.
- [9] Private Communication, Bill Ard, McDonnell Douglas Missile Systems Company.